Science of the Total Environment 648 (2019) 1002–1017

Contents lists available at ScienceDirect

Science of the Total Environment

journal homepage: www.elsevier.com/locate/scitotenv

Exploration of the effects of storm surge on the extent of saltwater intrusion into the surficial aquifer in coastal east-central Florida (USA)

Han Xiao [a,*], Dingbao Wang [a], Stephen C. Medeiros [a], Matthew V. Bilskie [b], Scott C. Hagen [b], Carlton R. Hall [c]

[a] Department of Civil, Environmental, and Construction Engineering, University of Central Florida, 12800 Pegasus Drive, ENGR II 324, Orlando, FL, United States of America
[b] Department of Civil and Environmental Engineering, Center for Computation & Technology, Center for Coastal Resiliency, Louisiana State University, Baton Rouge, LA, United States of America
[c] Ecological Program, Integrated Mission Support Services, Kennedy Space Center, Florida, United States of America

HIGHLIGHTS

- Storm surge from tropical cyclones can cause saltwater intrusion into coastal aquifers.
- Infiltrated saltwater can be diluted and flushed by infiltrated rainwater.
- Recovery of groundwater quality by infiltrated rainwater might need eight years.

GRAPHICAL ABSTRACT

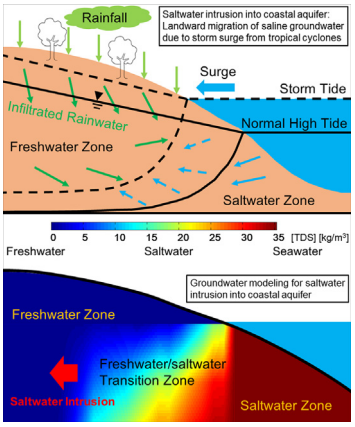

ARTICLE INFO

Article history:
Received 26 June 2018
Received in revised form 2 August 2018
Accepted 15 August 2018
Available online 17 August 2018

Editor: José Virgílio Cruz

Keywords:
Numerical modeling
SEAWAT
Saltwater intrusion
Surficial aquifer
Coastal east-Central Florida

ABSTRACT

Climate change such as altered frequency and intensity of storm surge from tropical cyclones can cause saltwater intrusion into coastal aquifers. In this study, a reference SEAWAT model and a diagnostic SEAWAT model are developed to simulate the temporal variation of surficial aquifer total dissolved solids (TDS) concentrations after the occurrence of a storm surge for exploration of the effects of storm surge on the extent of saltwater intrusion into the surficial aquifer in coastal east-central Florida (USA). It is indicated from the simulation results that: (1) rapid infiltration and diffusion of overtopping saltwater resulting from storm surge could cause a significant and rapid increase of TDS concentrations in the surficial aquifer right after the occurrence of storm surge; (2) rapid infiltration of freshwater from rainfall could reduce surficial aquifer TDS concentrations beginning from the second year after the occurrence of storm surge in that the infiltrated rainwater could generate an effective hydraulic barrier to impede further inland migration of saltwater and provide a downgradient freshwater discharge for saltwater dilution and flushing counteracting the effects of storm surge on the extent of saltwater intrusion; and (3) infiltrated rainwater might take approximately eight years to dilute and flush the overwhelming majority of infiltrated saltwater back out to the surrounding waterbodies, i.e., the coastal lagoons and the Atlantic Ocean.

* Corresponding author.
E-mail address: Han.Xiao@Knights.ucf.edu (H. Xiao).

https://doi.org/10.1016/j.scitotenv.2018.08.199
0048-9697/

1. Introduction

Saltwater intrusion (SWI) occurs as a result of the landward shift of the dynamic equilibrium between saline and fresh coastal groundwater usually caused by coastal aquifer overexploitation, and is a significant growing problem globally with detrimental effects such as reduction of fresh groundwater storage, degradation of drinking water quality and soil salinization, deserving of close attention in coastal areas around the world (Bear, 1979; Bear et al., 1999; Freeze and Cherry, 1979; Werner et al., 2013). Recently, studies focusing on assessments of the impacts of climate change on SWI into coastal aquifers blossomed, since climate change such as sea-level rise, changing groundwater recharge rates due to changing temperature and precipitation regimes, and increases in both the frequency and intensity of extreme weather events such as tropical storms and hurricanes can further increase the extent of SWI posing a significant challenge for coastal engineering and drinking water resource management in vulnerable coastal areas (Chang et al., 2011; Chui and Terry, 2013; Colombani et al., 2016; Intergovernmental Panel on Climate Change, 2007; Kazakis et al. 2016 & 2018; Langevin et al., 2005; Oude Essink et al., 2010; Ptak et al., 2011; Rasmussen et al., 2013; Sulzbacher et al., 2012; Tang et al., 2013; Werner and Simmons, 2009; Xiao et al., 2016; Yang et al. 2013 & 2015; Yu et al., 2016). For example, Chang et al. (2011) used numerical method based on SEAWAT computer code to evaluate the short-term and long-term impacts of sea-level rise on SWI into a conceptual unconfined and confined aquifer system; Chui and Terry (2013) conducted a numerical study to investigate the effects of eustatic sea-level rise on SWI into fresh groundwater lenses on a typical atoll in the tropical Pacific Ocean; Colombani et al. (2016) used numerical method based on SEAWAT computer code to quantify the foreseeable impacts of climate change on SWI into the unconfined aquifer of the Po Delta located in the coastal floodplain of the Po River in Northern Italy; Kazakis et al. (2016) used the electrical resistivity tomography (ERT) method in conjunction with hydro-chemical data to determine the extent and geometrical characteristics of SWI into the coastal aquifer of the eastern Thermaikos Gulf located in northern Greece; Kazakis et al. (2018) used the fuzzy logic based modification of the GALDIT method to assess the SWI vulnerability of coastal aquifers of Anthemountas basin located in Northern Greece; Langevin et al. (2005) developed an integrated surface-water/groundwater flow and solute transport model and applied it to the southern Everglades of Florida (USA) to assess the effects of hydro-climatologic conditions changes on SWI into the coastal aquifer; Oude Essink et al. (2010) constructed a three-dimensional numerical model to quantify the possible impacts of climate change in combination with anthropogenic activities on increasing the salinity level of the coastal groundwater system in the low-lying Dutch Delta in coastal Netherland; Rasmussen et al. (2013) used numerical method based on SEAWAT computer code to assess the impacts of sea-level rise and changes in groundwater recharge on SWI into the coastal aquifer of an island located in the Western Baltic Sea; Sulzbacher et al. (2012) implemented a numerical, density-dependent FEFLOW model to estimate climate change impacts on increasing the salinity level of the coastal aquifer of the North Sea Island of Borkum (Germany); Werner and Simmons (2009) developed two conceptual models to explore the extent of SWI into conceptual coastal unconfined aquifers in response to sea-level rise; Yang et al. (2013 & 2015) numerically investigated the impacts of tides and storm surges on changing coastal flow dynamics and alteration of salt distribution in the coastal aquifer situated north of Bremerhaven, northern Germany; Yu et al. (2016) simulated the impacts of coastal topographic features and increases in the frequency and intensity of storm surges on groundwater salinization in a conceptual coastal aquifer in coastal Delaware (USA).

Bilskie et al. (2014) and Passeri et al. (2015a, 2015b) demonstrated that the low-lying coastal alluvial plains and barrier islands in coastal east-central Florida (USA) are morphologically sensitive to changing hydrologic conditions associated with sea-level rise and increased intensity and frequency of storm surge from tropical cyclones, with the dynamic impacts including coastline erosion and SWI that result in alterations of the distribution and productivity of vegetation communities such as shifts in species composition possibly from less salt tolerant species to more salt tolerant species. Thus, in order to produce climate change adaptation strategies for tackling the issue of potential SWI, it is necessary to develop knowledge on the responses of coastal aquifer salinity to sea-level rise and the increase in intensity and frequency of storm surge from tropical cyclones. The complex nature of variable-density groundwater flow and solute transport in the low-lying coastal alluvial plains and barrier islands in coastal east-central Florida requires the use of numerical methods to simulate SWI (Anderson and Woessner, 1991), and the SEAWAT computer code (Guo and Langevin, 2002) that has been successfully applied to many case studies around the world (Cobaner et al., 2012; Langevin, 2003; Lin et al., 2009; Qahman and Larabi, 2006; Rasmussen et al., 2013; Sanford and Pope, 2010) is selected as the simulation code in this study.

In the low-lying coastal alluvial plains and barrier islands in coastal east-central Florida, the effects of sea-level rise on the extent of SWI into the surficial aquifer were quantitatively simulated by the SEAWAT models developed by Xiao et al. (2016), and the simulation results indicated that sea-level rise will play a vital role causing SWI. In this study, the objective is to develop SEAWAT models to simulate the effects of storm surge from tropical cyclones on the extent of SWI into the surficial aquifer of the low-lying coastal alluvial plains and barrier islands in coastal east-central Florida as a continuous study of Xiao et al. (2016) for exploration of the impacts of climate change (e.g., sea-level rise, storm surge, etc.) on the extent of SWI. In this study, a reference SEAWAT model and a diagnostic SEAWAT model are developed for quantifying the temporal variation of TDS concentrations in the surficial aquifer from the occurrence of storm surge to twenty years after its occurrence for exploring: (1) what is the extent of SWI into the surficial aquifer and how far inland the toe of the subterranean saltwater wedge can encroach?; and (2) how long it takes for the infiltrated saltwater to be diluted and flushed from the surficial aquifer by infiltration of freshwater from rainfall?.

2. Overview of study area

2.1. Site description

The study area is the Cape Canaveral Barrier Island Complex (CCBIC) area located in the low-lying coastal alluvial plains and barrier islands in coastal east-central Florida, consisting of multiple barrier islands, saltwater/freshwater lagoons, and the Atlantic Ocean coastline. The CCBIC area covers an area of approximately 1000 km^2 bounded by the Atlantic Ocean to the east, Mosquito Lagoon to the northeast and north, Indian River Lagoon to the west, and Banana River to the southeast and south (Fig. 1a), and is recognized as having high biodiversity because of the unique transitional geographic setting between the Caribbean and Carolinian zoogeographic provinces (Hall et al., 2014). The topographic variation is relatively small since the region is mainly composed of broad flat lowlands, and the land surface elevation varies from −0.2 to 10 m with a regional average of about 1.2 m NAVD 88 (LiDAR data from the National Aeronautics and Space Administration (NASA)).

2.2. Hydro-climatic conditions

The climate is humid subtropical with hot/humid summers (mean temperature varying from 22 °C to 33 °C) and mild/dry winters (mean temperature varying from 10 °C to 22 °C) with a mean annual rainfall of 1366 mm (annual rainfall varying from 848 mm to 2075 mm) (Mailander, 1990). The regional hydrologic conditions are characterized by dynamic interactions between surface water and groundwater, evapotranspiration, and rainfall (Hall et al., 2014; Schmalzer et al., 2000) as shown in Fig. 1b. Water levels in the coastal lagoons are

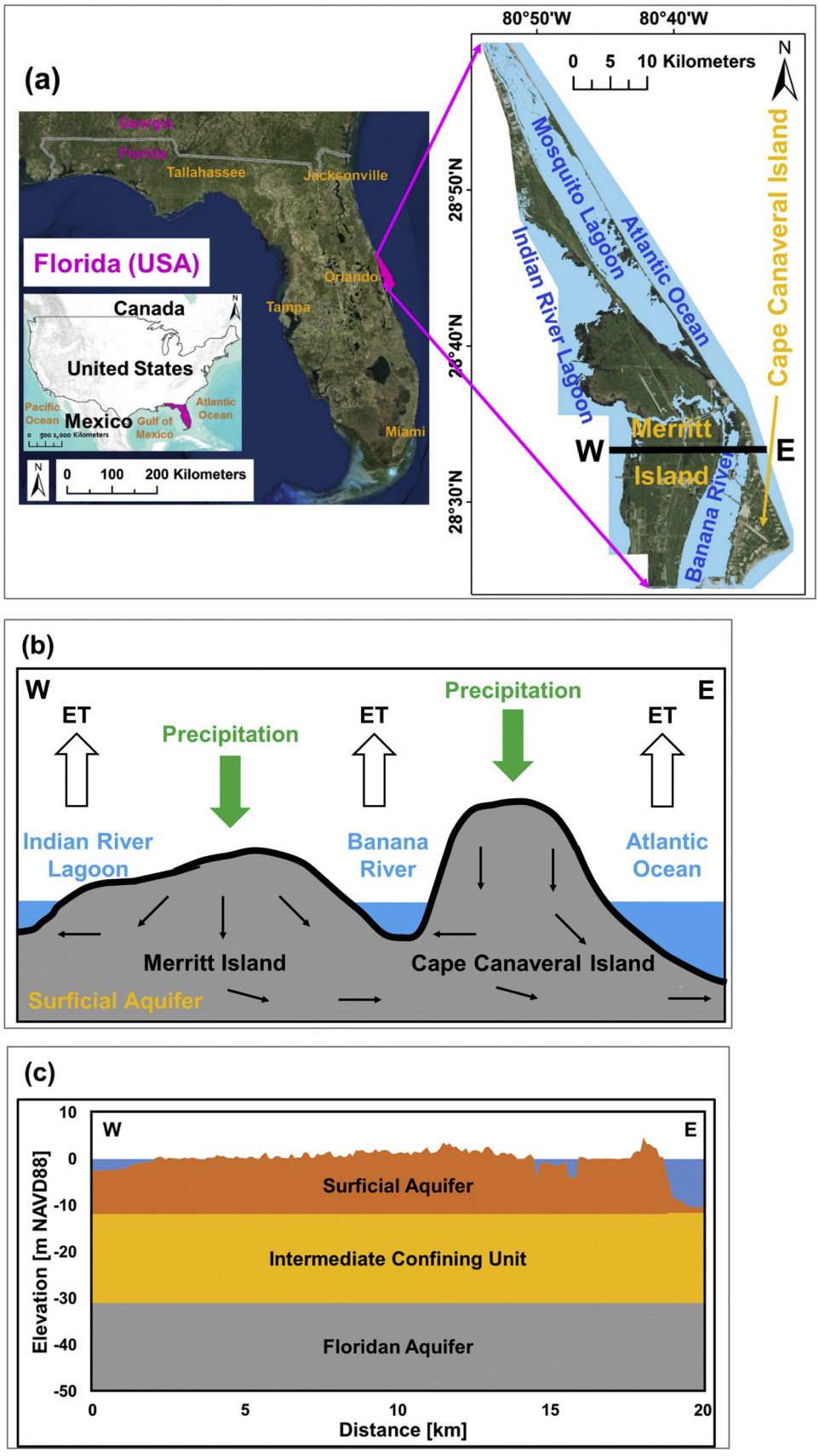

Fig. 1. a Location of the CCBIC area; **b** Illustration of the hydrologic conditions of the CCBIC area (west to east cross-section labeled W-E); **c** Hydrogeologic cross-section (west to east cross-section labeled W-E) of the coastal aquifer (note that only a small portion of the Floridan aquifer is shown since its bottom is much deeper than −50 m (NAVD88)).

dominated by the annual rise and fall of sea level with a maximum of near 0 m (NAVD88) in October. Water flow between the coastal lagoons is primarily driven by wind forcing. In most places, the coastal lagoons have a shallow, flat seagrass covered bottom with an average depth of 1.5 m, and are micro-tidal (1–2 cm) due to the narrow and distant inlet connections to the Atlantic Ocean. The TDS concentration typically varies from 10 to 45 kg/m^3.

2.3. Hydrogeologic settings

The hydrostratigraphic units are composed of, from top to bottom, the surficial aquifer, the intermediate confining unit, the Floridan aquifer, and the lower confining unit as shown in Fig. 1c, and the characteristics of each hydrostratigraphic unit are described in details in Williams and Kuniansky (2016), Miller (1986), and Schmalzer and Hinkle (1990), and are briefly described in Table 1.

The surficial aquifer occurs in the saturated part of the moderate- to low-permeability Holocene and Pleistocene sediments of fine to medium sand, coquina, silt, shell and marl, and is mainly composed of fine to medium sand which has the water table as its upper boundary and the top of the intermediate confining unit as its lower boundary. The primary inflow is infiltrated rainwater and the primary outflow is evapotranspiration and discharge to surface water bodies, i.e., fresh and/or salty marshes/wetlands, coastal lagoons and the Atlantic Ocean. The water table, which rises to its highest level late in the wet season (September) and drops to its lowest level late in the dry season (April), is mainly controlled by the temporal variation of rainfall and the seasonal thermal expansion and contraction of the Atlantic Ocean (Foster et al., 2017). The saltwater/freshwater transition zone formed in the coastal areas migrates either landward (saltwater intrusion) or seaward (saltwater recession) in correspondence with the lowering or rising water table, and its thickness is mainly dependent on the characteristics of the hydrogeologic settings. The focus of this study is to simulate the temporal variation of TDS concentrations in the surficial aquifer and explore the extent of SWI into the surficial aquifer in that the surficial aquifer: (1) is highly vulnerable to storm surge induced SWI; (2) plays a crucial role in the interaction of surface water and groundwater; (3) supports marshes/wetlands and provides groundwater discharge to the surrounding coastal lagoons and the Atlantic Ocean; and (4) is extremely important to the bio-diversity ecosystem and the survival of the threatened and endangered species of wildlife. Exploration of the effects of storm surge on SWI into the Floridan aquifer is not conducted in this study because the Floridan aquifer is highly mineralized which greatly limits its consumptive use.

2.4. Storm surge from tropical cyclones

The effects of storm surge associated with Hurricane Jeanne (a category 5 tropical cyclone swept a storm surge across the Caribbean area in middle and late September 2004) are explored in this study. Hurricane Jeanne, a storm of exceptionally large size and strength, was deemed the deadliest hurricane in the 2004 Atlantic hurricane season (Demotech Inc., 2014). The storm passed over the Caribbean area including Puerto Rico, Dominican Republic, Haiti, and the Bahamas beginning on Sep. 13th, 2004, and eventually made landfall near Stuart, Florida, approximately 150 km south of the CCBIC area, on September 25th, 2004, as a Category 3 hurricane. Hurricane Jeanne caused 5 direct deaths and $6.8 billion in property damage in the mainland US which made it the 13th costliest hurricane in US history (Lawrence and Cobb, 2005) at the time. Storm surge up to 2 m associated with Hurricane Jeanne occurred along the Florida east (Atlantic) coast. Florida's west (Gulf of Mexico) coast experienced a negative storm surge of about 1.4 m below normal tides when wind was blowing offshore, followed by a positive storm surge of about 1.1 m above normal tides when wind was blowing onshore at Cedar Key, Florida (http://www.stormsurge.noaa.gov/event_history_2000s.html). The near-term effects of the storm surge associated with Hurricane Jeanne including loss of human life and property damage were devastating; however, the long-term effects on coastal water resources, vegetation communities and wildlife habitat were also catastrophic as well. Coastal saltwater/freshwater marshes/wetlands were flooded both during and up to several days after the storm surge. Undoubtedly, coastal lowlands with flat topography and shallow water table depths such as those found in the CCBIC area experienced saltwater overtopping during surge events that subsequently resulted in increases in groundwater salinity, surficial soil salinization and vertical SWI. Potential consequences of exposure to the overtopping saltwater also included the shift of marshes from fresh or less saline to brackish or saline marshes, vegetation species dieback and limited recovery (or shift in vegetation species composition from less to more salt-tolerant species), and reduction in biomass production (Steyer et al., 2007).

The time-variant water levels of the coastal lagoons and the Atlantic Ocean, as well as the height of overtopping seawater in coastal lowlands during the storm surge associated with Hurricane Jeanne are simulated by a two-dimensional, unstructured finite-element storm surge model implemented by ADCIRC (Matthew V. Bilskie, Louisiana State University, unpublished data, 2016). The simulation of the ADCIRC storm surge model (astronomic tides and waves not considered) with a minimum element size of 10 m within the CCBIC area starts the day before

Table 1
A brief description of the hydrostratigraphic units of the CCBIC area and its vicinity.

Geologic age	Stratigraphic unit		Hydro-stratigraphic unit	Thickness (m)	Lithological character	Water-bearing property
Holocene and Pleistocene	Holocene and Pleistocene deposits		Surficial aquifer system (SAS)	0–33	Fine to medium sand, sandy coquina and sandy shell marl	Low permeability, yields small quantity of water
Pliocene	Pliocene and upper Miocene deposits		Intermediate confining unit	6–27	Gray sandy shell marl, green clay, fine sand and silty shell	Very low permeability
Miocene	Hawthorn Formation		(ICU)	3–90	Sandy marl, clay, phosphorite, sandy limestone	General low permeability, yields small quantity of water
Eocene	Ocala Group	Crystal River Formation	Floridan aquifer system	0–30	Porous coquina in soft and chalky marine limestone	General very high permeability, yields large quantity of artesian water
		Williston Formation	(FAS)	3–15	Soft granular marine limestone	
		Inglis Formation		>21	Coarse granular limestone	
	Avon Park Formation			>87	Dense chalky limestone and hard, porous, crystalline dolomite	
Paleocene	Cedar Keys Formation		Lower confining unit (LCU)	–	Interbedded carbonate rocks and evaporites	Very low permeability

Hurricane Jeanne made landfall on Florida's east coast (Sep. 23rd, 2004) and terminates after Hurricane Jeanne passed over Florida and shifted to Georgia and South Carolina (Sep. 28th, 2004). During the entire six-day storm surge simulation, the 'effective' simulation lasts for 84 h (3.5 days) beginning when sea level increases are observable and ending when sea levels return to their basis, and the simulation results are shown in Fig. 2. The simulated time-variant water surface elevations of the coastal lagoons and the Atlantic Ocean before, during, and after the occurrence of the storm surge associated with Hurricane Jeanne are used to develop the SEAWAT models for exploring the effects of storm surge on the extent of SWI into the surficial aquifer.

3. Numerical modeling

3.1. Model development

In this study, a reference SEAWAT model and a diagnostic SEAWAT model are developed to explore the effects of storm surge on SWI into the surficial aquifer in coastal east-central Florida CCBIC area.

3.1.1. Reference model

The reference model is implemented using SEAWAT to simulate the annual-averaged steady-state surficial aquifer TDS concentrations before the occurrence of storm surge. Due to the lack of surficial aquifer salinity measurements, the simulated TDS concentrations are unable to be calibrated. Instead, the simulated groundwater hydraulic heads are calibrated against the field-measured groundwater hydraulic heads (from observation wells). The simulated TDS concentrations from the calibrated reference model are visualized using ArcGIS to show the surficial aquifer TDS concentrations before the occurrence of storm surge.

3.1.2. Diagnostic model

The diagnostic model is implemented using SEAWAT to simulate the temporal variation of surficial aquifer TDS concentrations after the occurrence of storm surge (simulation period from the time of its occurrence to twenty years after its occurrence). The reference model serves as the 'baseline' model, and the diagnostic model is implemented based on the calibrated reference model. Compared to the reference model, the temporal discretization is switched from steady-state to transient and the boundary condition representing the water levels of the coastal lagoons and the Atlantic Ocean is converted from constant head boundary to time-variant specified head boundary to enable simulations of both rapid and long-term responses of aquifer salinity to storm surge, while other model input including the spatial discretization, the aquifer parameters, and the boundary conditions representing recharge, evapotranspiration, lateral head-dependent and bottom no-flux hydrologic boundaries remained unchanged, based on the assumption that all of the other hydrologic/hydrogeologic conditions are not affected by storm surge. Due to the transitory nature of storm surge, the rapid-response sampling of water table depth and TDS concentration in the influenced areas is not feasible, hence the implemented diagnostic model is not able to be calibrated. The output of the diagnostic model is visualized in ArcGIS to show the temporal variation of surficial aquifer TDS concentrations after the occurrence of storm surge.

Note that the impacts of other climate change factors such as sea-level rise and changes of temperature and precipitation regimes, as well as the impacts of astronomic tides are not taken into consideration in this study. The impacts of tidal fluctuations on groundwater levels and TDS concentrations are usually limited to the recirculating zone that is located very close to shoreline (salt concentration in the recirculating zone may vary due to tidal activities) (Narayan et al., 2007; Yang et al., 2013). However, the impacts of tidal activities during tide cycle on the fluctuation of saltwater/freshwater interface and saltwater wedge and on the migration of saltwater/freshwater transition zone are very small and are usually considered to be negligible (Werner et al., 2013; Yang et al., 2013). Moreover, the tidal amplitude in the study area is relatively small at just millimeters in range (micro-tidal) because: (1) tidal flows within the coastal lagoons are especially damped due to the limited inlets choking the tides entering the coastal lagoons; and (2) tidal energy is greatly dissipated due to the expansive size and shallowness of the estuary (Bilskie et al., 2017). Therefore, the impacts of astronomic tides are not taken into account in this study.

3.2. Spatial discretization

The determination of horizontal and vertical discretization that can effectively represent the topographic variation of land surface and the dimension and movement of saltwater/freshwater transition zone is of great importance, and the criterion is to enhance simulation accuracy using finer discretization but to maintain reasonable computer runtimes.

3.2.1. Reference model

Horizontally, a uniform grid spacing of 100 m in both the x- and y-directions is assigned (646 rows and 373 columns) to the model domain as shown in Fig. 3a. Vertically, the model domain is divided into five layers as shown in Fig. 3b. The top elevation of Layer 1 is set to the land-surface/sea-floor elevation (LiDAR DEM from the National Aeronautics and Space Administration (NASA) as shown in Fig. 4a) and the bottom elevation of Layer 1 is set to −2 m (NAVD 88). From Layers 2 to 5, the layers are flat and have a uniform thickness of 2 m. The bottom elevation of Layer 5 is set to the surficial aquifer bottom elevation (−10 m NAVD88) (Schmalzer et al., 2000).

3.2.2. Diagnostic model

Compared to the reference model, the horizontal and vertical discretization of the diagnostic model is exactly the same with the reference model.

3.3. Temporal discretization

3.3.1. Reference model

The reference model is a steady-state model which simulates the annual-averaged steady-state TDS concentrations in the surficial aquifer based on the assumptions that: (1) climate change impacts such as sea-level rise and storm surge are negligible; and (2) the groundwater systems are in 'equilibrium' with the annual-averaged steady-state hydroclimatic conditions.

Further temporal discretization is introduced in terms of transport time steps for better simulation of salinity transport. The length of the transport time step is specified to start with 0.01 day and increased by a time step multiplier of 1.2, with a maximum transport time step of 100 days. The program does not terminate until steady-state is reached.

3.3.2. Diagnostic model

Compared to the reference model (steady-state), the diagnostic model is transient which simulates the temporal variation of surficial aquifer TDS concentrations after the occurrence of storm surge. The diagnostic model starts from Sep. 25th, 2004 to Sep. 26th, 2024, and the 20-year simulation period is divided into 15 stress periods. Stress Periods 1 to 14 are within the time period of the storm surge event starting from Sep. 25th, 2004 to Sep. 27th, 2004 when water levels of the coastal lagoons and Atlantic Ocean were varied, while Stress Period 15 starts when water surface elevations returned back to normal on Sep. 27th, 2004 and terminates 20 years later on Sep. 26th, 2024. From Stress Periods 1 to 14, each stress period has a uniform length of 6 h with a constant time step length of 0.1 h (6 min). For Stress Period 15, the stress period length is designated to be 7305 days (approximately 20 years) with a minimum and a maximum time step lengths of 0.1 day and

30 days (starting from 0.1 day with a time step multiplier of 1.2), respectively.

3.4. Parameters

3.4.1. Reference model

The hydrogeologic parameters including horizontal/vertical hydraulic conductivity, porosity, longitudinal/transverse/vertical dispersivity, and diffusion coefficient are tabulated in Table 2.

3.4.2. Diagnostic model

Compared to the reference model, the hydrogeologic parameters of the diagnostic model are exactly the same with the reference model.

3.5. Boundary conditions

For minimizing the boundary effects, the model domain extends offshore to simulate the surface water and groundwater interactions between the surficial aquifer and coastal lagoons as well as the Atlantic Ocean. The constant head and concentration boundary, the time-variant specified head and concentration boundary, the no-flow boundary, the general-head boundary, the well boundary, the recharge boundary, and the evapotranspiration boundary are used for implementing the reference model and the diagnostic model.

3.5.1. Reference model

The constant head and concentration boundary is assigned to the coastal lagoons and the Atlantic Ocean for representing the water levels and the TDS concentrations. The water levels of the coastal lagoons and the Atlantic Ocean are obtained from observations, and the TDS concentrations of the coastal lagoons and the Atlantic Ocean is assumed to be equal to the seawater TDS concentration (35 kg/m^3) due to a lack of in-situ TDS concentration measurements (Sharqawy et al., 2010). The horizontal view of the constant head and concentration boundary assigned to Layer 1 is shown in Fig. 4b. The no-flow boundary is assigned to the lateral boundaries in Layers 1, 2, 3, 4, and 5 where groundwater flux through the boundaries is zero, and is also assigned to the bottom of Layer 5 since groundwater flux between the surficial

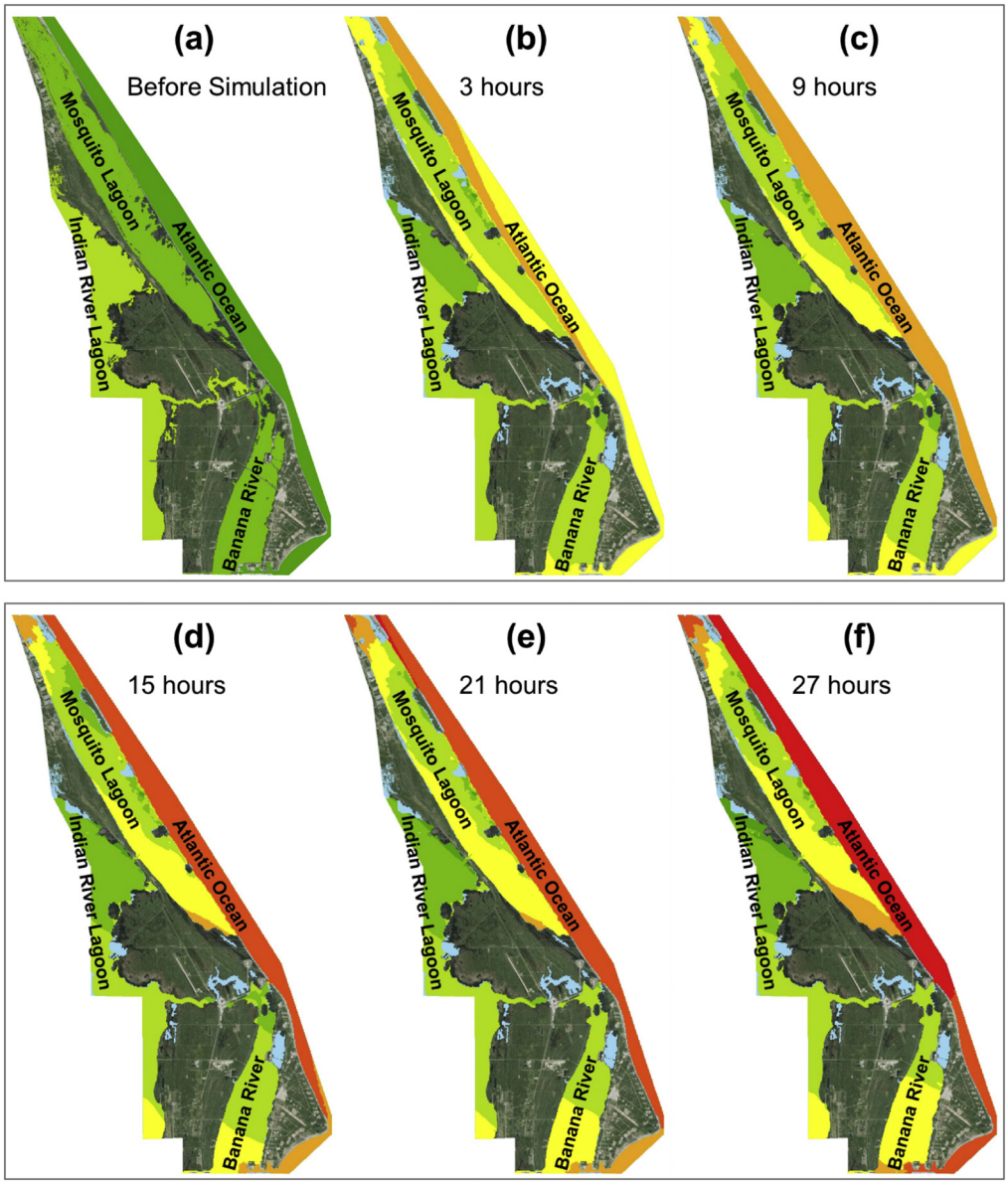

Fig. 2. Time-variant water surface elevations [m NAVD88] of the coastal lagoons and the Atlantic Ocean before, during, and after 8 ADCIRC simulation: **a** Before simulation; **b** 3 h; **c** 9 h; **d** 15 h; **e** 21 h; **f** 27 h; **g** 33 h; **h** 39 h; **i** 45 h; **j** 51 h; **k** 57 h; **l** 63 h; **m** 69 h; **n** 75 h; **o** 81 h; **p** After simulation.

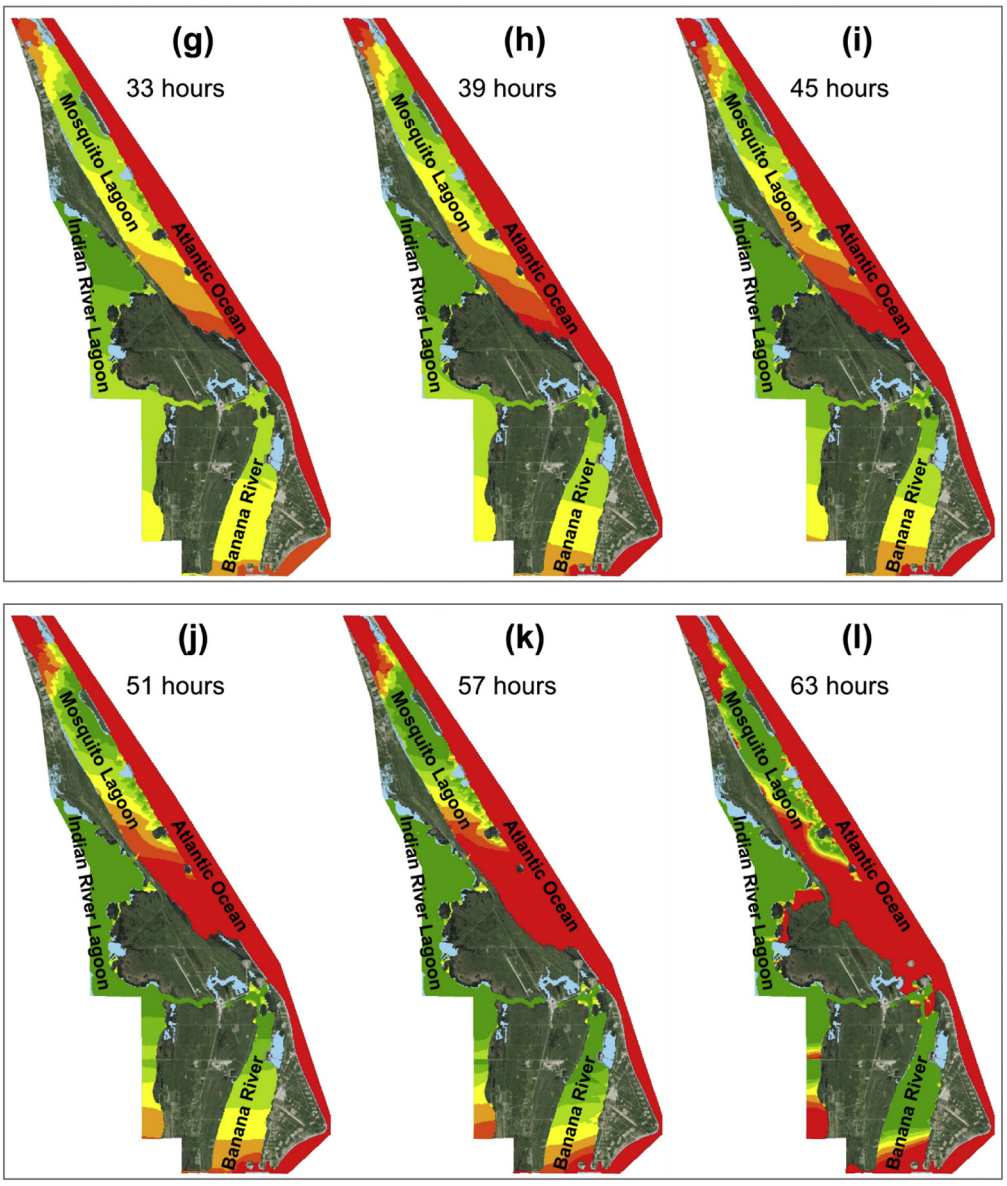

Fig. 2 (*continued*).

aquifer and the underlying Floridan aquifer through the intermediate confining unit is negligible (Schmalzer et al., 2000). The general-head boundary is assigned to the lateral boundaries in Layers 1, 2, 3, 4, and 5 where groundwater flux through the boundaries is non-zero for representing groundwater inflow and outflow. The well boundary is assigned to the groundwater pumping wells for representing groundwater abstraction from the surficial aquifer. The recharge boundary is assigned to the top of Layer 1 for representing infiltration from rainfall (Fig. 4c), and the evapotranspiration boundary is assigned to the top of Layer 1 for representing groundwater evaporation and plant transpiration.

3.5.2. Diagnostic model

Compared to the reference model, the constant head boundary representing the water levels of the coastal lagoons and the Atlantic Ocean is replaced by the time-variant specified head boundary since the water levels are varied during the time period of storm surge. All of the other boundary conditions are exactly the same with the reference model based on the assumption that other hydro-climatic/hydrologic conditions remain unchanged. The time-variant water levels assigned to the time-variant specified head boundary are from the output of the storm surge ADCIRC model (Matthew V. Bilskie, Louisiana State University, unpublished data, 2016), and the time-variant specified head boundary assigned to Layer 1 is shown in Fig. 2.

3.6. Initial conditions

3.6.1. Reference model

Accurate starting heads and concentrations (starting heads and concentrations consistent with the designated aquifer properties and boundary conditions) are not required since the reference model is a steady-state model. Reasonable estimations of the starting heads and concentrations based on the observed data are used as the initial conditions to avoid numerical instability during simulation.

3.6.2. Diagnostic model

Unlike steady-state simulation, transient simulation requires accurate starting heads and concentrations. Thus, the output of the calibrated reference model (groundwater hydraulic heads and TDS concentrations) is used as the initial conditions before starting the

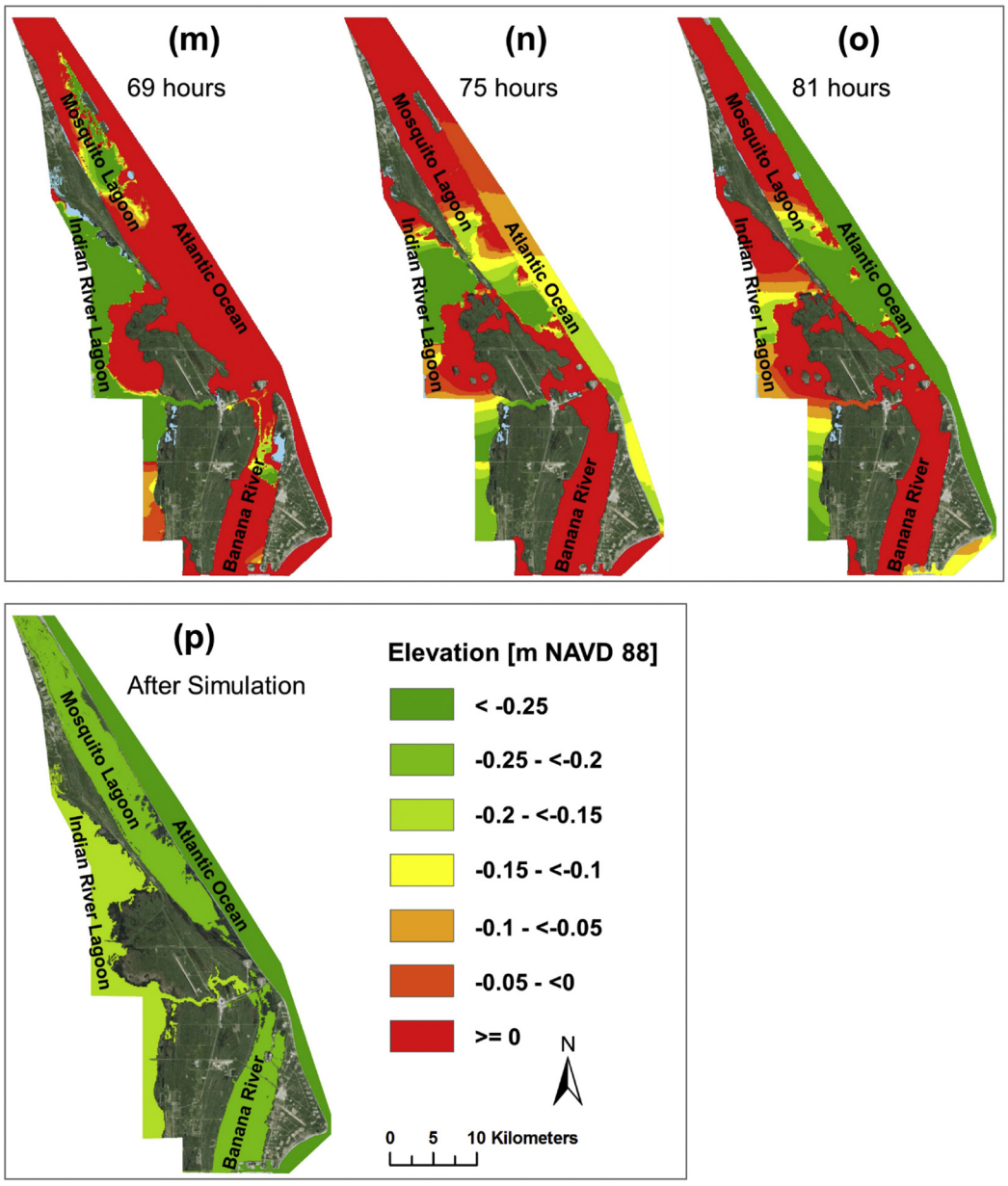

Fig. 2 (*continued*).

simulation of Stress Period 1. From Stress Periods 2 to 15, the output of the previous stress period simulation is used as the initial conditions for the current stress period simulation. For example, the output of Stress Period 2 simulation is used as the initial conditions for Stress Period 3 simulation.

4. Results and interpretation

4.1. Calibration

As mentioned above, the TDS concentrations simulated by the reference model are not able to be calibrated because of the lack of groundwater salinity measurements. Instead, the hydraulic heads simulated by the reference model are calibrated against the field-measured groundwater levels from the observation wells.

There are 10 active observation wells located within the CCBIC area monitoring daily variation of water table elevations during the time period from 2006 to 2014 as shown in Fig. 5a. Daily water table elevations monitored by each observation well from 2006 to 2014 are averaged to compute the annual-averaged steady-state water table elevations, and the calculated water table elevations serve as the calibration targets. During the calibration process, the horizontal and vertical hydraulic conductivities are adjusted using a trial-and-error method aiming at minimizing the differences between the simulated hydraulic heads (output from Layer 1 of the reference model) and the monitored water table elevations (calibration targets). The calibration process does not terminate until the simulated heads match the observed water table elevations to a satisfactory degree.

After calibration, the Nash-Sutcliffe model efficiency (NSE) coefficient reaches 0.96 (Fig. 5b), demonstrating a good agreement between the simulated and the observed groundwater hydraulic heads and indicating a good model performance. To further determine the model performance, the concepts of 'simulated' and 'true' marshes/wetlands are introduced herein. The 'simulated' marshes/wetlands refer to: (1) the land areas that have simulated water table elevations higher than land surface elevations; and (2) the land areas that have simulated water table elevations lower than land surface elevations but the simulated water table depths are <0.2 m. The 'true' marshes/wetlands refer to

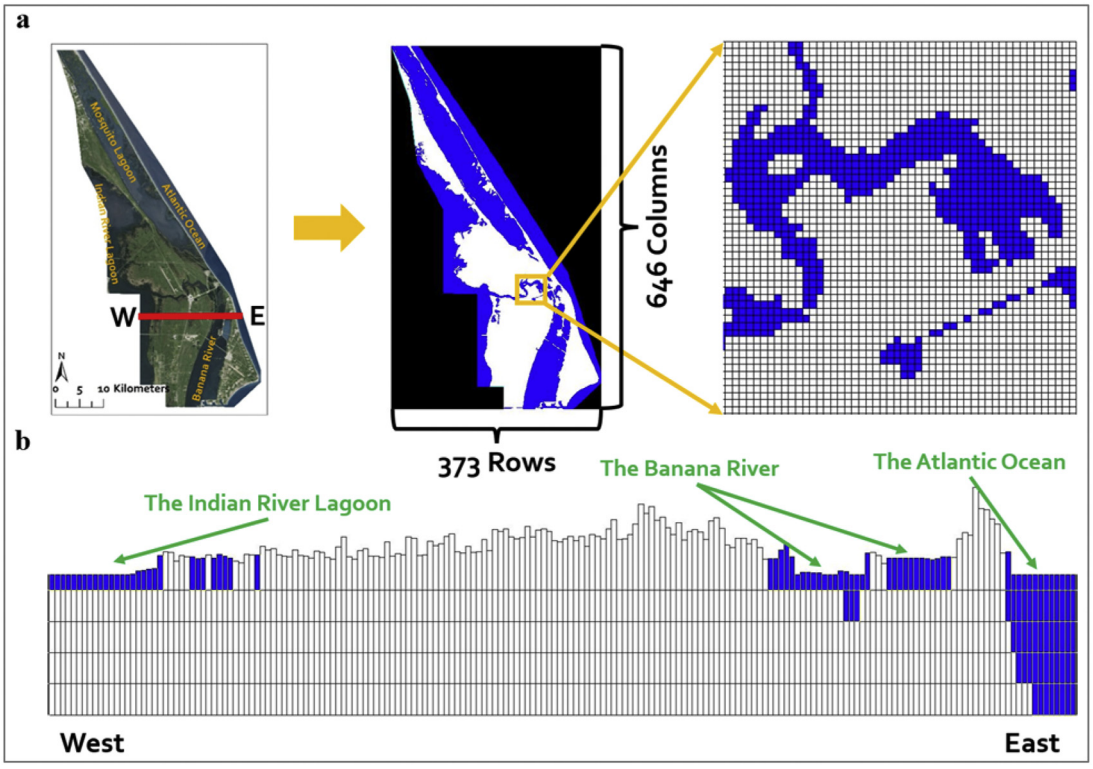

Fig. 3. Spatial discretization: **a** Plan view; **b** Cross-sectional view (W-E).

the marshes/wetlands classified by the map of land use and land cover in 2009 provided by the St. Johns River Water Management District (http://www.sjrwmd.com/gisdevelopment/docs/themes.html). The comparison between the 'simulated' and 'true' marshes/wetlands is shown in Fig. 5c. By conducting a statistical analysis, the percentage of consistency is calculated to be 64.6%, demonstrating a good agreement between the 'simulated' and 'true' marshes/wetlands and indicating a good model performance.

Note that marshes/wetlands are complicated and dynamic natural systems composed of swamps, marshes, and bogs dependent not only on water table depth but also topography, vegetation cover and soil type. Thus, it is not optimal to define the concept of "simulated" marshes/wetlands solely based on water table depth. However, the comparison between the 'simulated' and 'true' marshes/wetlands is worthwhile since the calibration targets are limited. It is also expected that field measurements of groundwater hydraulic heads and TDS concentrations would be available in future for further calibration.

4.2. Spatial and temporal variation of TDS concentrations

The TDS concentrations in the saltwater/freshwater transition zone are higher than freshwater ([TDS] no >1 kg/m^3) and lower than seawater ([TDS] equal to 35 kg/m^3), and the saltwater/freshwater transition zone is further categorized as slightly saline zone ([TDS] varying from

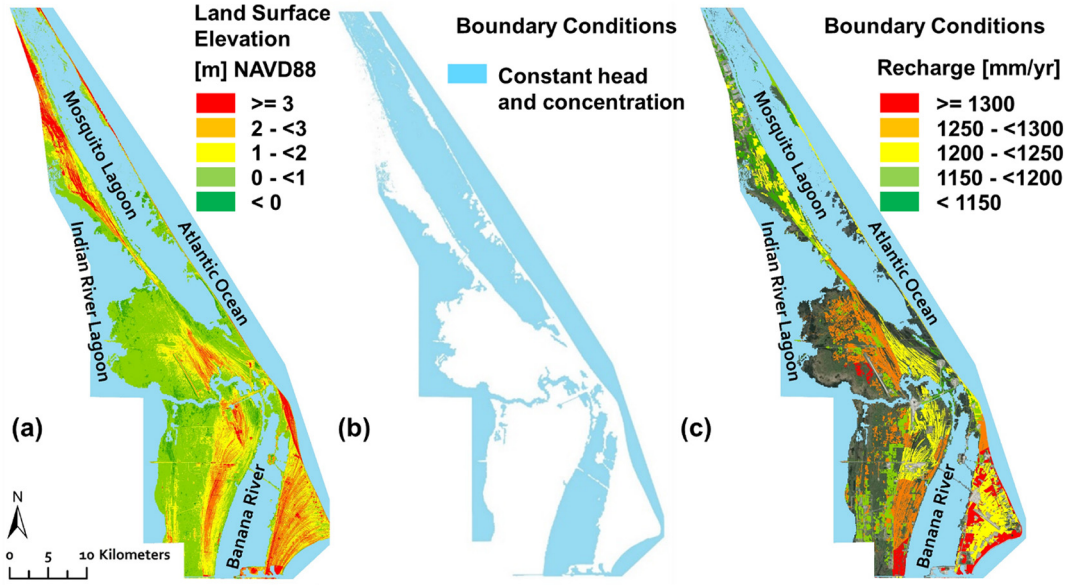

Fig. 4. a Land surface elevation (m NAVD 88) from LiDAR data; **b** Constant head and concentration boundary assigned to Layer 1; **c** Recharge boundary assigned to Layer 1.

Table 2
Hydrogeologic parameters.

Hydrogeologic parameters	Value [units]	References
Horizontal hydraulic conductivity (K_h)	15 [m/d]	McGurk and Presley, 2002
Anisotropy (K_h/K_z)	10 [−]	
Porosity (n)	0.2 [−]	Blandford et al., 1991
Longitudinal dispersivity (a_L)	6 [m]	Hutchings et al., 2003
Transverse dispersivity (a_T)	0.01 [m]	
Vertical dispersivity (a_V)	0.025 [m]	
Diffusion coefficient (D^*)	0.00128 [m^2/d]	

1 to 3 kg/m^3), moderately saline zone ([TDS] varying from 3 to 10 kg/m^3), and highly saline zone ([TDS] varying from 10 to 35 kg/m^3) based on the TDS concentrations (NGWA, 2010). In this study, contours of 1, 3, 10 and 35 kg/m^3 TDS concentrations are used to determine the location and migration of the transition zone for the exploration of the extent of SWI. Note that the simulated TDS concentrations are from Layer 1 of the reference model and the diagnostic model.

4.2.1. Reference model

The simulated surficial aquifer TDS concentrations before the occurrence of storm surge are shown in Fig. 6. From the plan view (Fig. 6a), the transition zone is mainly located at the western CCBIC area where the saltwater wedge toe trespasses 3–4 km inland. From the vertical view along the N-S transect (Fig. 6b), the widths of the slightly saline zone and the moderately saline zone are relatively thin, while the width of the highly saline zone is thick.

4.2.2. Diagnostic model

The plan view of the temporal variation of the simulated surficial aquifer TDS concentrations after the occurrence of storm surge is shown in Fig. 7.

From Fig. 7a, the saltwater/freshwater transition zone is mainly located at the coastal low-lying areas (average land surface elevation varying from −0.1 to 0.2 m NAVD88) classified as fresh marsh, intermediate marsh (less saline than brackish), brackish marsh and saline marsh (map of land use and land cover in 2009 provided by the St. Johns River Water Management District) in the west-central and east-central CCBIC area adjacent to the Indian River Lagoon and the Atlantic Ocean. Due to low altitude and flat topography, storm surge from tropical cyclones can push seawater laterally inland approximately 4–5 km, resulting in large amounts of those coastal low-lying areas being overtopped by seawater. The overtopping seawater can infiltrate into the unsaturated zone rapidly, developing salt plumes moving downwards vertically to water table and contaminating surficial aquifer, resulting in a severe extent of SWI. However, due to sufficient rainfall and high aquifer permeability, the dilution of the infiltrated saltwater is also rapid because a high rate of fresh groundwater recharge from infiltrated rainwater can generate a downgradient groundwater flow contributing to transporting saltwater back out to the surrounding waterbodies, i.e., the coastal lagoons and the Atlantic Ocean. Therefore, the severe extent of SWI is alleviated rapidly and the dilution/flushing rate is: (1) relatively fast in the first stage (from 2005 to 2011) as shown in Fig. 7b-h; and (2) relatively slow in the second stage (from 2012 to 2024) as shown in Fig. 7i-n. After the first and second stages, large amounts of saltwater has discharged to the surrounding water bodies, and the residual infiltrated saltwater still remains in the dilution phase while the dilution/flushing rate is very slow.

In Fig. 7, the temporal variation of the locations of the saltwater/freshwater transition zone are highlighted. An expansion of the highlighted areas indicates inland migration of the transition zone, while a contraction of the highlighted areas indicates seaward migration of the transition zone. The covering area of the highlighted areas, the percentages of the covering area of the highlighted areas, and the percentages increases of the covering area of the highlighted areas are calculated and tabulated in Table 3. Besides, the percentages increases of the covering area of the highlighted areas are plotted in Fig. 8.

The percentage increase of the covering area of the highlighted areas is zero before the occurrence of storm surge (Sep. 25th, 2004), and increases significantly to 18.79% right after the occurrence of storm surge. Then, the percentage increase curve remains rising until the

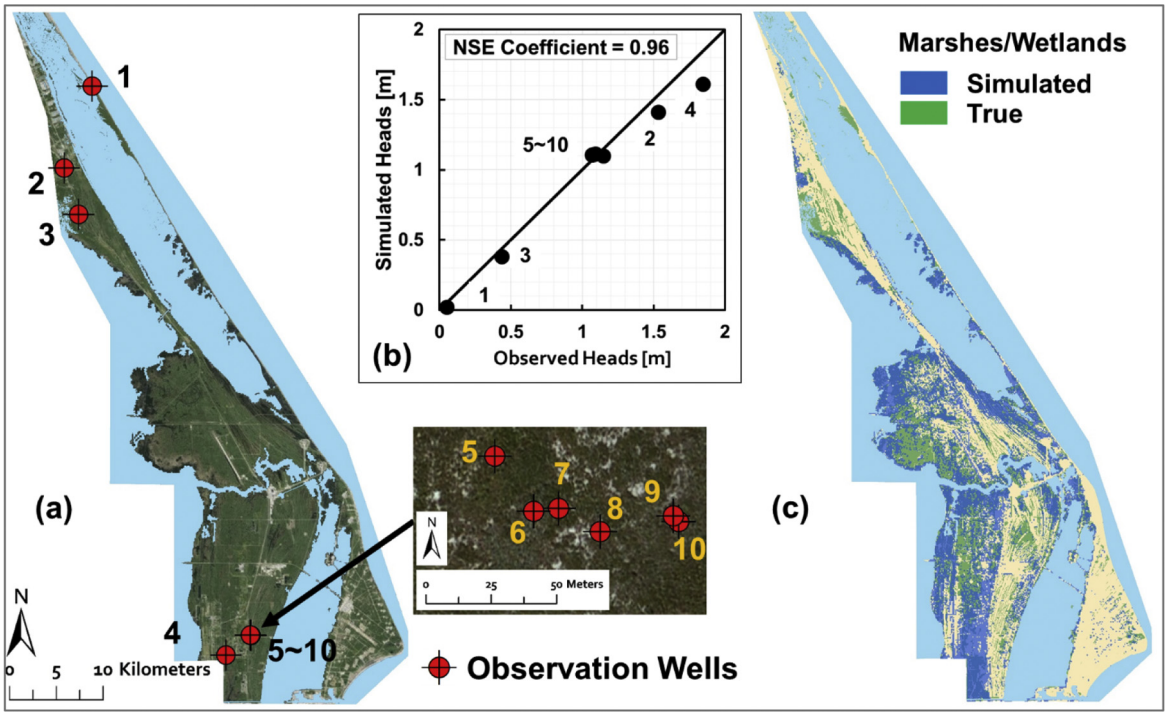

Fig. 5. a Location of the 10 active observation wells; **b** Scatter diagram showing the goodness of fit between the observed and simulated heads; **c** Comparison between the 'simulated' and 'true' marshes/wetlands.

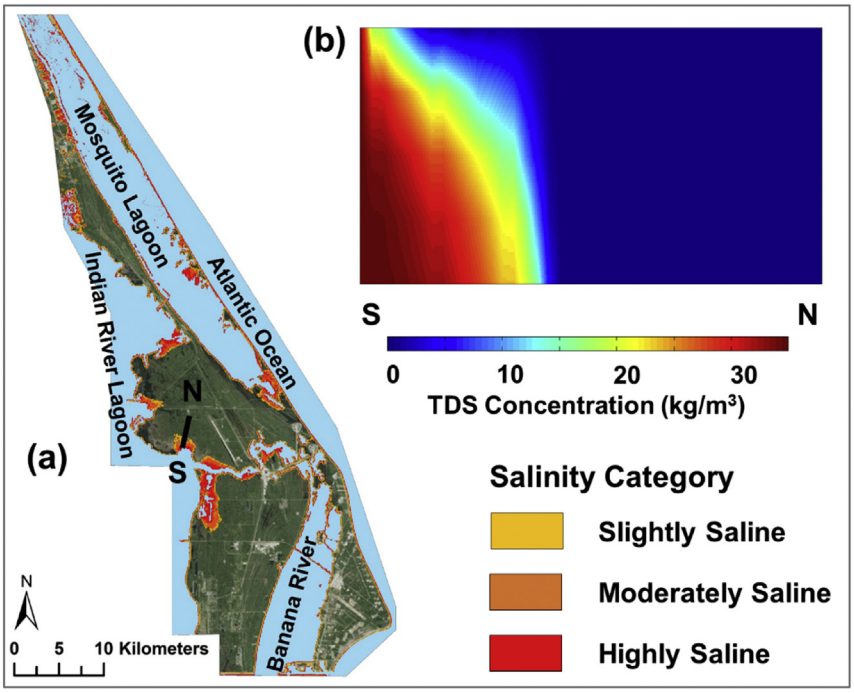

Fig. 6. Surficial aquifer TDS concentration before storm surge: **a** Plan view; **b** South to north cross-sectional view.

peak is reached (19.42%) on May 25th, 2005. Afterwards, the percentage increase curve starts to decline following a first-order exponential decay curve generally. From the years of 2005 to 2011, the decline rate of the percentage increase curve is relatively fast (annual decline rate approximately 2.70%), indicating that large amounts of infiltrated saltwater is diluted and flushed back to the surrounding water bodies. From the years of 2012 to 2024, the decline rate of the percentage increase curve is relatively slow (annual decline rate approximately 0.16%), indicating that the dilution/flushing process continues at a much slower rate and the surficial aquifer TDS concentrations returns back to normal gradually. Based on the percentage increase curve, it is estimated that it might take approximately eight years for the infiltrated rainwater to dilute and flush the overwhelming majority of the infiltrated saltwater back out to the surrounding waterbodies, i.e., the coastal lagoons and the Atlantic Ocean. However, it might still take several years for an "entire" recovery of the surficial aquifer water quality.

5. Discussion

The effects of storm surge from tropical cyclones on the extent of SWI into the surficial aquifer are a major concern to the local ecosystem in the CCBIC area. Storm surge sweeping over the CCBIC area can cause saltwater overtopping on coastal lowlands in that waves can reach and pass over the crest of the coastal defense structure (dunes) if wave run-up and storm tide levels are high enough (EurOtop, 2007). After storm surge has receded, stagnant seawater that trapped in the topographic depressions in the coastal low-lying areas can act as effective point-sources of contamination because ponding saltwater can infiltrate into the porous media rapidly, while open wells existing in the coastal lowlands can greatly expedite the rapid vertical transmission of saltwater, resulting in SWI into the surficial aquifer (Vithanage et al., 2012).

Immediately after the occurrence of storm surge, the infiltrated saltwater forms a layer of denser fluid above the lighter freshwater layer, and the formed saltwater plume is "forced" downgradient (seaward) by infiltrated rainwater to the surrounding water bodies, i.e., the coastal lagoons and the Atlantic Ocean, resulting in a reduction of surficial aquifer TDS concentrations which is referred to natural remediation of coastal aquifer water quality (Steyer et al., 2007). Usually, the natural remediation process takes several months to several years, dependent on aquifer permeability and hydro-climatic conditions (Yang et al. 2013 & 2015). The natural remediation process could be fast if the aquifer permeability is high and rainfall is sufficient, while the natural remediation process could be slow if the aquifer permeability is low and rainfall is insufficient. From the simulation results, it is estimated that the natural remediation process might take approximately eight years (Fig. 8). In comparison to the recovery time of the coastal aquifers of the Pukapuka Atoll (approximately one year) in the Northern Cook Islands (South Pacific Ocean) which suffered from tropical cyclone Percy (Category 5) in late February 2005 (Terry and Falkland, 2010), the recovery time of the surficial aquifer in the CCBIC area is much longer (approximately eight years) primarily because of the amounts of infiltrated rainfall and aquifer permeability. First, the permeability of the surficial aquifer in the CCBIC area is an order of magnitude lower than the permeability of the coastal aquifers in the Pukapuka Atoll. Second, the long-term records of the annual-averaged rainfall of the CCBIC area is approximately 1366 mm, which is less than one half of the annual-averaged rainfall of the Pukapuka Atoll (approximately 2860 mm). Third, the storm surge swept the CCBIC area in late September near the end of the wet season immediately prior to the dry season. During the seven-month dry season (from October to April), dilution/flushing of the infiltrated saltwater by infiltrated rainwater is limited, while the extent of SWI into the surficial aquifer aggravates due to continuous infiltration/diffusion of the overtopping saltwater. It is very likely that the natural remediation process might be faster and the recovery time might be shorter if the storm surge struck the CCBIC area earlier in the wet season, say May or June, since high rate of freshwater infiltration caused by large rainfall/storms later in the wet season could contribute to saltwater dilution/flushing.

Although it is estimated that natural remediation process might take approximately eight years to reduce increasing salinity back to normal conditions, however, the increasing salinity within the eight years could have a long-term environmental impacts in the CCBIC area. Increasing salinity can create problems for plant species by altering their metabolic pathways and rates of activities, and the influences in the CCBIC area can be at small or large scales dependent on the magnitude of the changes in salinity level. Salt tolerance of plant communities

depends on plant species, duration and degree of exposure to increasing salinity, salinity increasing rate, and mineral content of soil, and some plant species can tolerate a wide range of salinity and can recover soon once salinity declines while some plant species cannot tolerate increasing salinity and cannot recover even if salinity declines afterwards (Howard and Mendelssohn, 1999; Webb and Mendelssohn, 1996). Consequences of exposure to increasing salinity include, but are not limited to, alteration of the distribution and productivity of plant communities, dieback and limited recovery of plant species, shift in plant community compositions from less salinity-tolerant species to more salinity-tolerant species, and reduction in biomass production (Steyer et al., 2007). Besides, the coastal CCBIC area is mainly composed of fresh, intermediate (less saline than brackish), brackish, and saline marshes/wetlands, and increasing salinity at the traditional freshwater areas can cause a shift from fresh or less saline marshes/wetlands to brackish or saline marshes/wetlands. Moreover, increasing salinity could reduce citrus production, which is the main agricultural product in the CCBIC area. In addition, increasing salinity could affect water supply from abstraction wells for agricultural and domestic use, since upconing of deeper saltwater could occur and coastal wells are particularly at high risk of being submerged by overtopping saltwater.

As a supplement of natural remediation, the extent of SWI would be further compensated by artificial remediation. Oude Essink (2001) proposed five artificial mitigation approaches to prevent or to retard the SWI process, including: (1) implementing freshwater injection barriers through deep-well injection or infiltration of freshwater or reclaimed water near the shoreline; (2) extracting saline/brackish groundwater; (3) reducing groundwater withdrawal rates and/or relocation of coastal abstraction wells; (4) increasing artificial recharge in upland areas to enlarge submarined groundwater discharge to generate an effective hydraulic barrier for impeding further inland migration of saltwater and to provide a downgradient freshwater discharge for saltwater dilution and flushing; and (5) creating physical barriers such as sheet piles and clay trenches. Among these artificial mitigation measures, (1) and (4) might be effective to be applied in the CCBIC area. Besides, it is extremely important and necessary to prevent saltwater overtopping in

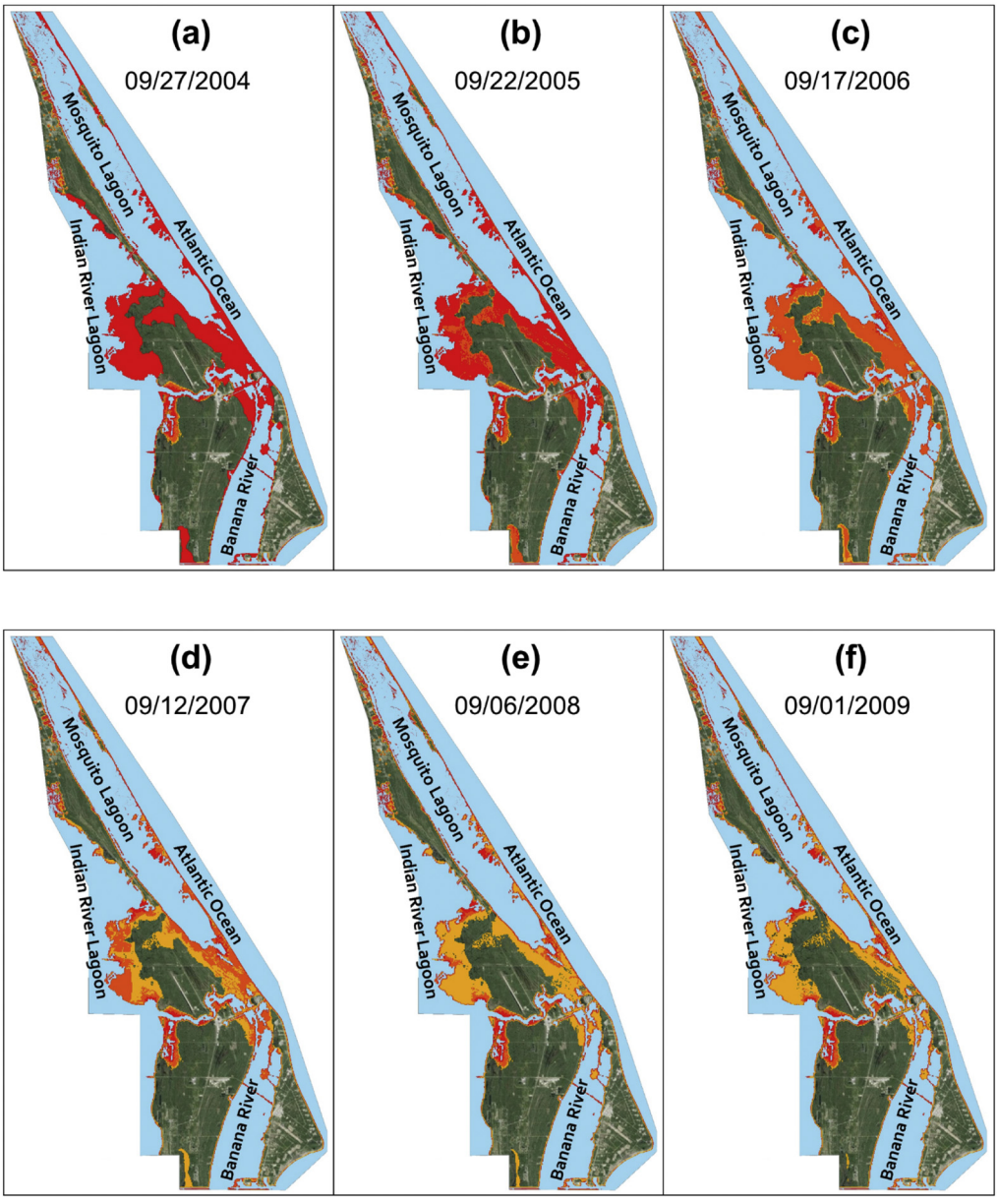

Fig. 7. Surficial aquifer TDS concentration after storm surge (plan view): **a** 09/27/2004; **b** 09/22/2005; **c** 09/17/2006; **d** 09/12/2007; **e** 09/06/2008; **f** 09/01/2009; **g** 09/01/2010; **h** 09/01/2011; **i** 08/31/2012; **j** 08/31/2013; **k** 08/31/2014; **l** 08/30/2016; **m** 08/29/2020; **n** 08/29/2024.

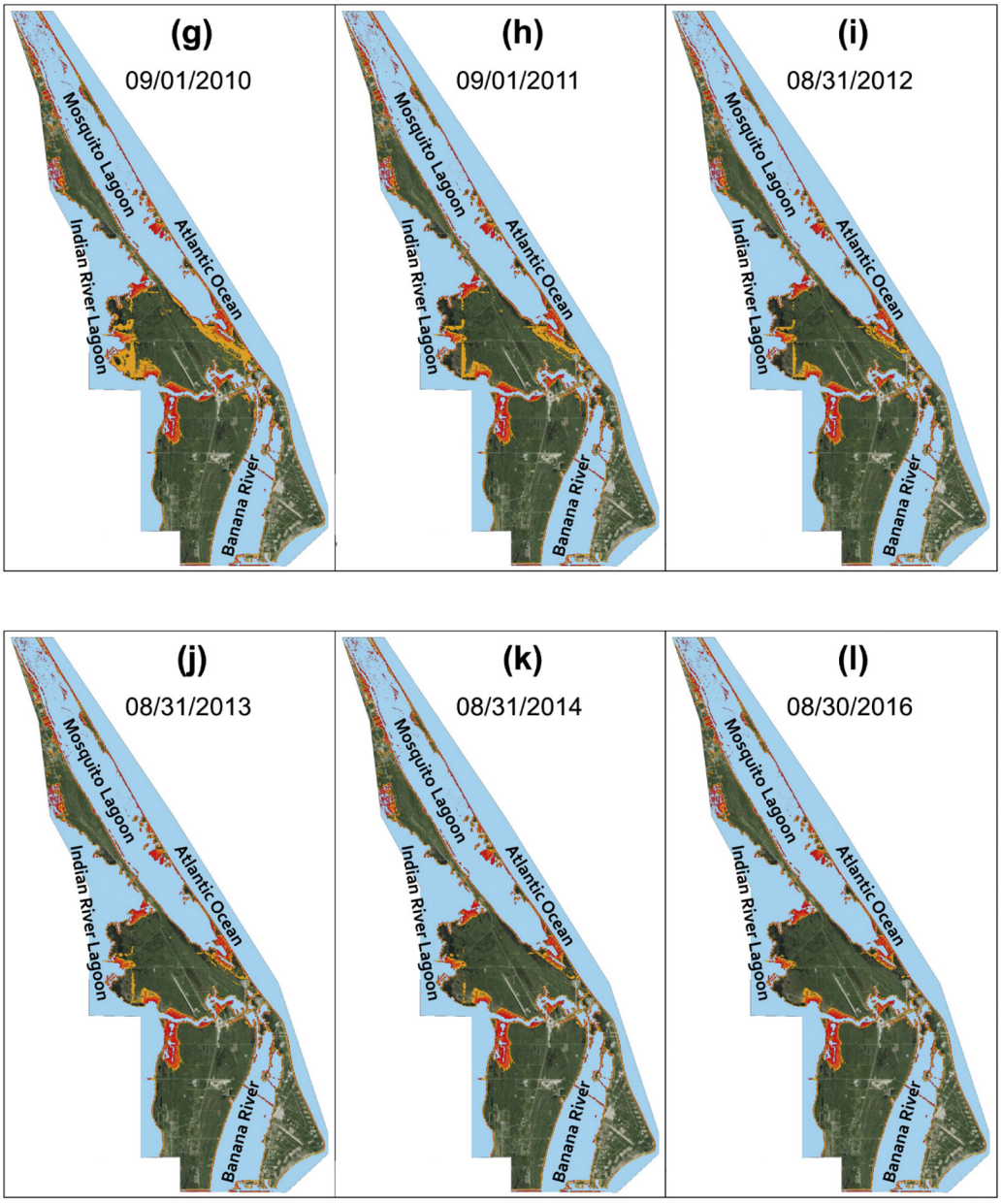

Fig. 7 (*continued*).

coastal low-lying areas for reducing the risk of saltwater infiltration/diffusion into the surficial aquifer. Construction and maintenance of artificial coastal defense structures such as seawalls might be a good choice to stabilize beach and shoreline and to protect coastal lowland from saltwater overtopping. However, the cost is usually expensive and it is not really necessary to build up breakwaters/seawalls that are primarily used to absorb shock of waves to protect coastline from high energy waves, since the study area is raw natural without man-made harbor, dock, or channel inlet/outlet. Thus, an economical but efficient measure could be to heighten and strengthen the existing sand dunes and build up "new" dunes where sand dunes are destroyed or missing near the shoreline so as to impede saltwater washing over coastal lowland caused by storm surge. It is expected that the extent of SWI could be greatly compensated if saltwater overtopping in coastal lowland does not occur.

The simulation results provide an initial exploration of the effects of storm surge from tropical cyclones on the extent of SWI into the surficial aquifer and estimation of the groundwater recovery time under natural remediation process, which is very useful for discussions of climate change adaptation planning and management in the CCBIC area and other similar environments worldwide. However, note that large uncertainties can be associated with the reference and diagnostic models, resulting in the simulation results a certain degree unreliable.

First, the lack of sufficient sampling data for calibration has the largest uncertain range and the largest effect on simulation results. As mentioned above, the simulated hydraulic heads output from the reference model are calibrated against the field-measured groundwater levels while the simulated TDS concentrations are not calibrated due to the lack of salinity measurements, whereas both the simulated hydraulic heads and TDS concentrations output from the diagnostic model are not calibrated due to the lack of groundwater level and salinity measurements. Even if it is feasible to implement a groundwater monitoring system within the study area now, it might not be practical to collect data for calibrating the diagnostic model since the storm surge is a past event occurred several years ago.

Second, the ignorance of spatial variation of hydrogeologic parameters (horizontal/vertical hydraulic conductivity, porosity, longitudinal/transverse/vertical dispersivity, and diffusion coefficient) has the

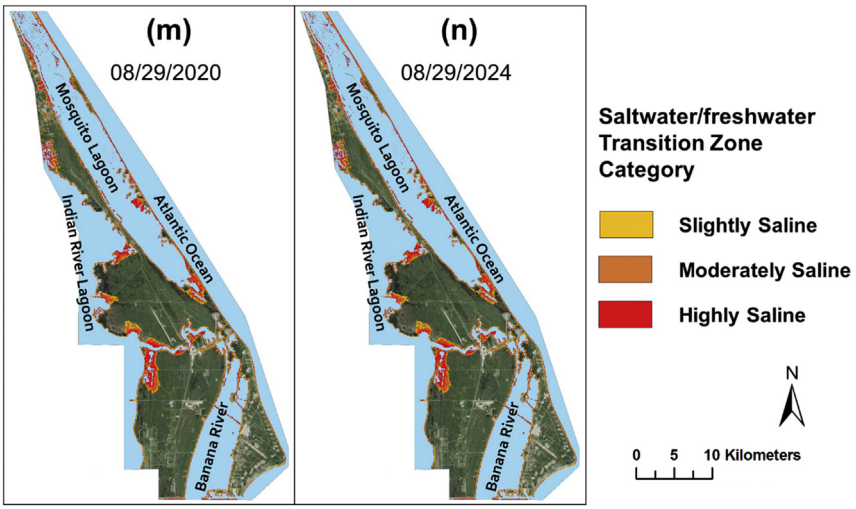

Fig. 7 (*continued*).

uncertain range and the effect on simulation results. Due to the lack of geophysical surveys and borehole tests, the spatial variation of hydrogeologic parameters are unknown, and the surficial aquifer is deemed as homogenous with uniform values initially assigned to all model grid cells expecting to be adjusted during calibration. The ignorance of the impact of heterogeneity of the surficial aquifer simplifies the model implementation while sacrifices the accuracy of the simulated salinity at local scale, but is considered to be appropriate and reasonable for implementation of a regional-scale model. The advantages of this 'simple' model implementation include, but are not limited to: (1) rendering the capability of implementing finer vertical discretization so that the vertical salinity gradient and the thickness and migration of saltwater/freshwater transition zone could be accurately simulated; (2) less computational demand and shorter computer runtime; and (3) lowering the risk of numerical instability.

Table 3
Percentage (increase) of the covering area of the highlighted areas.

Date	Covering area (km^2)	Percentage (%)	Percentage increase (%)
Before storm surge	69	13.55	–
Sep. 27th, 2004	165	32.34	18.79
Jan. 25th, 2005	168	32.83	19.28
May 25th, 2005	169	32.98	19.42
Sep. 22nd, 2005	168	32.96	19.41
Jan. 20th, 2006	168	32.83	19.28
May 20th, 2006	167	32.6	19.05
Sep. 17th, 2006	165	32.22	18.67
Jan. 15th, 2007	162	31.72	18.17
May 15th, 2007	159	31.14	17.59
Sep. 12th, 2007	156	30.59	17.04
Jan. 10th, 2008	153	29.92	16.36
May 9th, 2008	149	29.09	15.54
Sep. 6th, 2008	144	28.13	14.58
Jan. 4th, 2009	138	27.06	13.51
May 4th, 2009	133	26.07	12.51
Sep. 1st, 2009	128	25.09	11.53
Sep. 1st, 2010	99	19.4	5.85
Sep. 1st, 2011	86	16.75	3.2
Aug. 31st, 2012	81	15.77	2.22
Aug. 31st, 2013	77	15.11	1.56
Aug. 31st, 2014	75	14.64	1.09
Aug. 30th, 2016	73	14.26	0.71
Aug. 30th, 2018	72	14.1	0.55
Aug. 29th, 2020	72	14.04	0.49
Aug. 29th, 2022	71	13.97	0.41
Aug. 29th, 2024	71	13.91	0.36

Third, the assumptions made for model simplification have the uncertain range and the effect on simulation results. SWI is recognized as a complex hydrogeologic process due to the complex nature of variable-density conditions and changing climate, and several assumptions have to be made attempting to simplify the procedures of model implementation. Assumptions made for simplification include that: (1) surface runoff is negligible and the overtopping seawater infiltrates downwards vertically and reaches water table eventually; (2) the residual overtopping seawater is drained out after the 3.5-day effective storm surge duration so that the saltwater ponding depth is zero afterwards; (3) the inland encroachment of the coastline after the storm surge is negligible; (4) continuous sea-level rise and additional storm surges associated with other tropical cyclones under the complex changing climate are ignored; and (5) the effects of astronomic tides are negligible. With these assumptions mentioned above, (4) has the larger uncertain range and larger effect on simulation results than (1), (2), (3), and (5). Due to the El Niño conditions in a greenhouse-enhanced world, an increase in both the frequency and intensity of extreme weather events such as tropical storms and hurricanes, in combination with continuous sea-level rise, are expected to bring more frequent and intense storm surges to coastal areas (Van Biersel et al., 2007), with their magnitude dependent on the dynamics of storms, coastal topography, and the position of the coastline relative to the storm track (Bruss et al., 2011). Consequently, if stronger and more persistent El Niño conditions are projected for the Caribbean area over the next few years, the surficial aquifer of the CCBIC area will be under greater threat from storm surge and sea-level rise, as well as subsequent SWI of its limited freshwater resources. However, the assumptions described above are considered to be appropriate and reasonable for

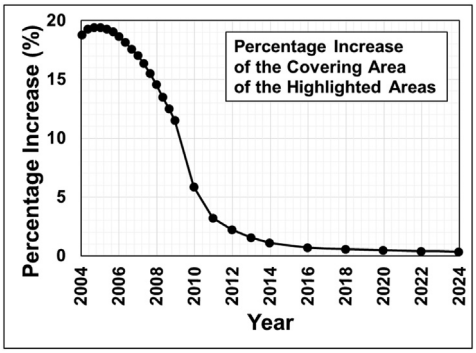

Fig. 8. Percentage increase of the covering area of the highlighted areas.

implementing a regional-scale model, whereas the interpretation of the simulation results to local scale might be limited to some extent.

As mentioned above, considerable uncertainties are introduced due to sampling data deficiencies and assumptions made for simplification of model implementation. Salinity level of the surficial aquifer is extremely important to the local bio-diversity ecosystem, and SWI can greatly threaten the survival of the endangered species of wildlife. Considering the importance of the surficial aquifer salinity level, the extent of SWI should be investigated periodically as the location and migration of the saltwater/freshwater transition zone may change with respect to time. Therefore, it goes without saying that implementing a continuous groundwater monitoring system for monitoring temporal variation of groundwater levels and TDS concentrations of the surficial aquifer, as well as conducting geophysical surveys and borehole tests for determination of soil characteristics are of great importance. From Fig. 5a, there are 10 active observation wells located within the CCBIC area monitoring daily variation of water table elevations during the time period from 2006 to 2014. However, these observation wells are located either at the northern or southern CCBIC area, while no observation well is installed at the central CCBIC area. Thus, construction of new observation wells at the central CCBIC area and its vicinity is essential so as to increase the representativeness of the collected data. Besides, hydro-geochemical analyses should be performed monthly, or at least twice per year (once at the end of wet season (September and/or October) and once at the end of dry season (April and/or May)). Further calibration for improving the accuracy of simulation results and reducing uncertainties would be feasible if such a groundwater monitoring system would be implemented and put into use and hydro-geochemical analyses would be conducted. In addition, to produce more reliable and adequate results of the extent of SWI, numerical modeling method can be used in combination with other techniques. For example, Kazakis et al. (2016) used electrical resistivity tomography (ERT) method in conjunction with hydro-geochemical data for mapping the extent and geometrical characteristics of SWI into the coastal aquifer of the eastern Thermaikos Gulf in northern Greece; Kazakis et al. (2018) modified the standard GALDIT method (the most established method worldwide used to assess the SWI vulnerability of coastal aquifer) using fuzzy multi-criteria categorization and proposed the GALDIT-F method and applied it to assess SWI vulnerability of the coastal aquifer of Anthemountas basin located in northern Greece. It is expected that numerical modeling method could be used in combination with the developed GALDIT and GALDIT-F methods, as well as the ERT technique to provide a comprehensive understanding of the complex process of SWI into the surficial aquifer in the CCBIC area.

6. Conclusion

Groundwater salinity is crucial in understanding both the short-term and long-term effects of the storm surge on coastal groundwater resources and ecosystem. The purpose of this study is to explore the effects of storm surge from tropical cyclones on the extent of SWI into the surficial aquifer of the CCBIC area located in the low-lying coastal alluvial plains and barrier islands in coastal east-central Florida, as well as estimating the recovery time required for infiltrated rainwater to dilute and flush infiltrated saltwater back out to the surrounding waterbodies, i.e., the coastal lagoons and the Atlantic Ocean. To achieve this goal, a reference SEAWAT model and a diagnostic SEAWAT model are developed in this study.

The results of this study contribute to ongoing research focused on forecasting vegetation community responses to climate change in the CCBIC area (Foster et al., 2017), and provide a useful reference for coastal groundwater resource management, land use planning, and ecosystem protection and restoration in a changing climate in the low-lying coastal alluvial plains and barrier islands in coastal east-central Florida and other similar environments worldwide as well. Future research will take into account the coupled effects of continuous sea-level rise, superposition of intensified storm surges due to multiple tropical cyclones, and changes of rainfall regimes to conduct a comprehensive assessment of climate change impacts on SWI into the surficial aquifer in coastal east-central Florida (USA).

Acknowledgements

This research was funded in part by the NASA Kennedy Space Center, Ecological Program, Climate Adaptation Science Investigators (CASI) Project (Award: IHA-SA-13-006) and the Louisiana Sea Grant Laborde Chair Endowment. The opinions, findings and conclusions expressed in this manuscript were those of the author(s) and not necessarily those of the NASA Kennedy Space Center or the Louisiana Sea Grant. The authors thank the editors and anonymous reviewers for their very constructive and insightful comments/suggestions on the earlier version of this manuscript. The authors also thank the NASA Kennedy Space Center Ecological Program, the U.S. Geological Survey, and the St. Johns River Water Management District for providing relevant data to conduct this research.

References

Anderson, M.P., Woessner, W.W., 1991. Applied Groundwater Modeling: Simulation of Flow and Advective Transport. Academic Press.
Bear, J., 1979. Hydraulics of Groundwater. McGraw-Hill.
Bear, J., Cheng, A., Sorek, S., Ouazar, D., Herrera, I., 1999. Seawater Intrusion in Coastal Aquifers: Concepts, Methods and Practices (Theory and Applications of Transport in Porous Media). Kluwer Academic Publishers.
Bilskie, M.V., Hagen, S.C., Medeiros, S.C., Passeri, D.L., 2014. Dynamics of sea level rise and coastal flooding on a changing landscape. Geophys. Res. Lett. 41 (3), 927–934.
Bilskie, M.V., Bacopoulos, P., Hagen, S.C., 2017. Astronomic tides and nonlinear tidal dispersion for a tropical coastal estuary with engineered features (causeways): Indian River lagoon system. Estuar. Coast. Shelf Sci. (in press).
Blandford, T.N., Birdie, T., Robertson, J.B., 1991. Regional Groundwater Flow Modeling for East-Central Florida with Emphasis on Eastern and Central Orange County. St. Johns River Water Management District Special Publication (SJ91-SP4).
Bruss, G., Gönnert, G., Mayerle, R., 2011. Extreme Scenarios at the German North Sea Coast: A Numerical Model Study. https://icce-ojs-tamu.tdl.org/icce/index.php/icce/article/download/1428/pdf_379.
Chang, S.W., Clement, T.P., Simpson, M.J., Lee, K., 2011. Does seal-level rise have an impact on saltwater intrusion? Adv. Water Resour. 34, 1283–1291.
Chui, T.F.M., Terry, J.P., 2013. Influence of sea-level rise on freshwater lenses of different atoll island sizes and lens resilience to storm-induced salinization. J. Hydrol. 502, 18–26.
Cobaner, M., Yurtal, R., Dogan, A., Motz, L.H., 2012. Three dimensional simulation of seawater intrusion in coastal aquifers: a case study in the Goksu deltaic plain. J. Hydrol. 464-465, 262–280.
Colombani, N., Osti, A., Volta, G., Mastrocicco, M., 2016. Impact of climate change on salinization of coastal water resources. Water Resour. Manag. 30, 2483–2496.
Demotech Inc., 2014. Impact of Storms on the Florida Property Insurance Market 1990–2003. Special Report. Demotech Inc. http://www.demotech.com/pdfs/papers/florida_cat_paper_20140723.pdf.
EurOtop, 2007. Manual on Wave Overtopping of Sea Defenses and Related Structures: An Overtopping Manual Largely Based on European Research, but for Worldwide Application. 2nd edition. http://www.overtopping-manual.com/docs/EurOtop%20II%202016%20Pre-release%20October%202016.pdf.
Foster, T.E., Stolen, E.D., Hall, C.R., Schaub, R., Duncan, B.W., Hunt, D.K., Drese, J.H., 2017. Modeling vegetation community responses to sea-level rise on Barrier Island systems: a case study on the Cape Canaveral Barrier Island complex, Florida, USA. PLoS One 12 (8), e0182605.
Freeze, R.A., Cherry, J.A., 1979. Groundwater. Prentice Hall.
Guo, W., Langevin, C.D., 2002. User's guide to SEAWAT: a computer program for simulation of three-dimensional variable-density ground-water flow. Techniques of Water-resources Investigations Book. 6.
Hall, C.R., Schmalzer, P.A., Breininger, D.R., Duncan, B.W., Drese, J.H., Scheidt, D.A., Lowers, R.H., Reyier, E.A., Holloway-Adkins, K.G., Oddy, D.M., Cancro, N.R., Provancha, J.A., Foster, T.E., Stolen, E.D., 2014. Ecological impacts of the space Shuttle Program at John F. Kennedy Space Center, Florida. NASA/TM-2014-216639. NASA, Washington, DC.
Howard, R.J., Mendelssohn, I.A., 1999. Salinity as a constraint on growth of oligohaline marsh macrophytes. I. Species variation in stress tolerance. Am. J. Bot. 86 (6), 785–794.
Hutchings, W.C., Tarbox, D.L., Engineers, H.S.A., 2003. A model of seawater intrusion in surficial and confined aquifers of northeast Florida. The 2nd International Conference on saltwater intrusion and coastal aquifers – monitoring, modeling, and management. http://www.olemiss.edu/sciencenet/saltnet/swica2/Hutchings_ext.pdf.
Intergovernmental Panel on Climate Change, 2007. IPCC Climate Change Synthesis Report: Summary for Policymakers. https://www.ipcc.ch/pdf/assessment-report/ar5/syr/AR5_SYR_FINAL_SPM.pdf.

Kazakis, N., Pavlou, A., Vargemezis, G., Voudouris, K.S., Soulios, G., Pliakas, F.K., Tsokas, G., 2016. Seawater intrusion mapping using electrical resistivity tomography and hydrochemical data. An application in the coastal area of eastern Thermaikos gulf, Greece. Sci. Total Environ. 543, 373–387.

Kazakis, N., Spiliotis, M., Voudouris, K.S., Pliakas, F.K., Papadopoulos, B., 2018. A fuzzy multicriteria categorization of the GALDIT method to assess seawater intrusion vulnerability of coastal aquifers. Sci. Total Environ. 621, 524–534.

Langevin, C.D., 2003. Simulation of submarine groundwater discharge to a marine estuary: Biscayne Bay, Florida. Ground Water 41 (6), 758–771.

Langevin, C.D., Swain, E., Wolfert, M., 2005. Simulation of integrated surface water/ground-water flow and salinity for a coastal wetland and adjacent estuary. J. Hydrol. 314, 212–234.

Lawrence, M.B., Cobb, H.D., 2005. Tropical Cyclone Report – Hurricane Jeanne, 13–28 September 2004. National Hurricane Center http://www.nhc.noaa.gov/data/tcr/AL112004_Jeanne.pdf.

Lin, J., Snodsmith, B., Zheng, C., Wu, J., 2009. A modeling study of seawater intrusion in Alabama Gulf Coast, USA. Environ. Geol. 57, 119–130.

Mailander, J.L., 1990. Climate of the Kennedy Space Center and vicinity. NASATech. Memo. 103498. NASA, Washington, DC.

McGurk, B., Presley, P.F., 2002. Simulation of the Effects of Groundwater Withdrawals on the Floridan Aquifer System in East-Central Florida: Model Expansion and Revision. St. Johns River Water Management District Technical Publication (SJ2002-5).

Miller, J.A., 1986. Hydrogeologic framework of the Floridan aquifer system in Florida and in parts of Georgia, Alabama, and South Carolina. U.S. Geological Survey Professional Paper 1403-B.

Narayan, K.A., Schleeberger, C., Bristow, K.L., 2007. Modeling seawater intrusion in the Burdekin Delta irrigation area, North Queensland, Australia. Agric. Water Manag. 89, 217–228.

NGWA, 2010. Brackish groundwater. National Groundwater Association Information Brief http://www.ngwa.org/mediacenter/briefs/documents/brackish_water_info_brief_2010.pdf.

Oude Essink, G.H.P., 2001. Improving fresh groundwater supply – problems and solutions. Ocean Coast. Manag. 44, 429–449.

Oude Essink, G.H.P., Van Baaren, E.S., PGB, De Louw, 2010. Effects of climate change on coastal groundwater systems: a modeling study in the Netherlands. Water Resour. Res. 46 (10), 5613–5618.

Passeri, D.L., Hagen, S.C., Bilskie, M.V., Medeiros, S.C., 2015a. On the significance of incorporating shoreline changes for evaluating coastal hydrodynamics under sea level rise scenarios. Nat. Hazards 75 (2), 1599–1617.

Passeri, D.L., Hagen, S.C., Medeiros, S.C., Bilskie, M.V., Alizad, K., Wang, D., 2015b. The dynamic effects of sea level rise on low-gradient coastal landscapes: a review. Earth's Future 3 (6), 159–181.

Ptak, T., Yang, M., Graf, J., Robert, T.M., 2011. A Modelling Study of Saltwater Iand Storm Surge Processes in Coastal Areas Under Climate Change, AGU Fall Meeting Abstract.

Qahman, K., Larabi, A., 2006. Evaluation and numerical modeling of seawater intrusion in the Gaza aquifer (Palestine). Hydrogeol. J. 14, 713–728.

Rasmussen, P., Sonnenborg, T.O., Goncear, G., Hinsby, K., 2013. Assessing impacts of climate change, sea level rise, and drainage canals on saltwater intrusion on coastal aquifer. Hydrol. Earth Syst. Sci. 17, 421–443.

Sanford, W.E., Pope, J.P., 2010. Current challenges using models to forecast seawater intrusion: lessons from the eastern shore of Virginia, USA. Hydrogeol. J. 18, 73–93.

Schmalzer, P.A., Hinkle, G.R., 1990. Geology, geohydrology and soils of Kennedy Space Center: a review. NASA Tech. Memo. 103813. NASA, Washington, DC http://ntrs.nasa.gov/archive/nasa/casi.ntrs.nasa.gov/19910001129.pdf.

Schmalzer, P.A., Hensley, M.A., Mota, M., Hall, C.R., Dunlevy, C.A., 2000. Soil, groundwater, surface water, and sediments of Kennedy Space Center, Florida: background chemical and physical characteristics. NASA/Technical Memorandum-2000-208583. NASA http://ntrs.nasa.gov/archive/nasa/casi.ntrs.nasa.gov/20000116077.pdf.

Sharqawy, M.H., Lienhard, J.H., Zubair, S.M., 2010. Thermophysical properties of seawater: a review of existing correlations and data. Desalin. Water Treat. 16, 354–380.

Steyer, G.D., Perez, B.C., Piazza, S.C., Suir, G., 2007. Potential consequences of saltwater intrusion associated with hurricanes Katrina and Rita: chapter 6C in science and the storms-the USGS response to the hurricanes of 2005. Circular, p. 1306-6C.

Sulzbacher, H., Wiederhold, H., Siemon, B., Grinat, M., Igel, J., Burschil, T., Günther, T., Hinsby, K., 2012. Numerical modelling of climate change impacts on freshwater lenses on the North Sea Island of Borkum using hydrological and geophysical methods. Hydrol. Earth Syst. Sci. 16, 3621–3643.

Tang, Y., Tang, Q., Tian, F., Zhang, Z., Liu, G., 2013. Responses of natural runoff to recent climatic variations in the Yellow River basin, China. Hydrol. Earth Syst. Sci. 17, 4471–4480.

Terry, J.P., Falkland, A.C., 2010. Responses of atoll freshwater lenses to storm-surge overwash in the northern Cook Island. Hydrogeol. J. 18, 749–759.

Van Biersel, T.P., Carlson, D.A., Milner, L.R., 2007. Impact of hurricane storm surges on the groundwater resources. Environ. Geol. 53, 813–826.

Vithanage, M., Engesgaard, P., Jensen, K.H., Illangasekare, T.H., Obeysekera, J., 2012. Laboratory investigations of the effects of geologic heterogeneity on groundwater salinization and flush-out times from a tsunami-like event. J. Contam. Hydrol. 136-137, 10–24.

Webb, E.C., Mendelssohn, I.A., 1996. Factors affecting vegetation dieback of an oligohaline marsh in coastal Louisiana – field manipulation of salinity and submergence. Am. J. Bot. 83 (11), 1429–1434.

Werner, A.D., Simmons, C.T., 2009. Impact of sea-level rise on sea water intrusion in coastal aquifers. Ground Water 47 (2), 197–204.

Werner, A.D., Bakker, M., Post, V.E.A., Vandenbohede, A., Lu, C., Ataie-Ashtiani, B., Simmons, C.T., Barry, D.A., 2013. Seawater intrusion processes, investigation and management: recent advances and future challenges. Adv. Water Resour. 51, 3–26.

Williams, L.J., Kuniansky, E.L., 2016. Revised hydrogeologic framework of the Floridan aquifer system in Florida and parts of Georgia, Alabama, and South Carolina (ver. 1.1, March 2016). U.S. Geological Survey Professional Paper 1807 (23 pls).

Xiao, H., Wang, D., Hagen, S.C., Medeiros, S.C., Hall, C.R., 2016. Assessing the impacts of sea-level rise and precipitation change on the surficial aquifer in the low-lying coastal alluvial plains and barrier islands, east-central Florida (USA). Hydrogeol. J. 24 (7), 1791–1806.

Yang, J., Graf, T., Herold, M., Ptak, T., 2013. Modelling the effects of tides and storm surges on coastal aquifers using a coupled surface-subsurface approach. J. Contam. Hydrol. 149, 61–75.

Yang, J., Graf, T., Ptak, T., 2015. Sea level rise and storm surge effects in a coastal heterogeneous aquifer: a 2D modelling study in northern Germany. Grundwasser 20, 39–51.

Yu, X., Yang, J., Graf, T., Koneshloo, M., O'Neal, M.A., Michael, H.A., 2016. Impact of topography on groundwater salinization due to ocean surge inundation. Water Resour. Res. 52, 5794–5812.